Lifetime of gap discrete breathers in diatomic crystals at thermal equilibrium

Liya Z. Khadeeva and Sergey V. Dmitriev
Institute for Metals Superplasticity Problems, Russian Academy of Sciences, Khalturin Street 39, Ufa 450001, Russia
(Received 28 March 2011; revised manuscript received 17 August 2011; published 17 October 2011)

Crystals having a gap in a phonon spectrum can support so-called gap discrete breathers (DBs), i.e., nonlinear localized vibrational modes existing in perfect crystals and having frequencies within the gap. In our recent work, for a two-dimensional crystal with stoichiometry A_3B, we have demonstrated that if the atomic weight of the components is related as $M_A \gg M_B$, then there is a wide gap in the phonon spectrum and the gap DBs can be easily excited. The situation is opposite if the above condition is not satisfied. In the present work the gap DBs are studied at thermal equilibrium, whereas in the previous study the temperature was zero. We demonstrate that in the crystal supporting DBs, in contrast to the opposite case, the lifetime of high-energy light atoms grows with temperature. The possible role of gap DBs in the thermally activated formation of vacancy and interstitial atom pairs (Frenkel pairs) was studied. We have measured the time needed for the appearance of a Frenkel pair as a function of temperature for the crystals supporting and not supporting DBs. A minor difference in waiting time of Frenkel pair nucleation was found in these two cases. We argue that, for the model and its parameters considered in the present work, the main mechanism of thermally activated Frenkel pair formation is the cooperative motion of atoms rather than the excitation of DBs.

DOI: 10.1103/PhysRevB.84.144304 PACS number(s): 05.45.Yv, 63.20.−e

I. INTRODUCTION

Discrete breathers (DBs) are spatially localized vibrational modes of high amplitude ubiquitous in discrete nonlinear systems.[1–4] DBs have been studied in connection to various fields of science, including condensed-matter physics,[5–12] nonlinear optics,[13] chains of superconducting Josephson junctions,[14] DNA models,[15] Bose-Einstein condensates,[16] materials science,[2,17] carbon nanotubes,[18,19] graphene,[20] etc.

Theoretical work by Sievers and Takeno[21] initiated the studies focused on rigorous proof that DBs are the exact solutions to various nonlinear discrete equations. Those studies, summarized in recent reviews (see, e.g., Ref. 1), led to a fundamental understanding of basic properties of DBs and conditions of their existence in nonlinear lattices.

Nowadays, the trend is toward the study of DBs in realistic systems. One of the main issues is experimental observation of DBs. This has been done for many discrete nonlinear systems,[1–4] including observation of gap DBs in thermodynamic equilibrium in a NaI crystal.[5,6] Properties of DBs in thermal equilibrium have been also studied numerically in two-dimensional monoatomic systems with hard and soft anharmonicities, taking into account only nearest-neighbor interactions.[22,23] The authors of these works have analyzed the power spectrum of crystals at thermal equilibrium and demonstrated that the lifetime of DBs increases with temperature growth.

Physical processes where DBs can play an essential role are under active discussion. Manley has described the mechanisms by which DBs can modify properties of materials.[2] Bishop *et al.* have studied the relaxor behavior of ferroelectric perovskite oxides, taking into account their inherent anharmonicity and the possibility to support DBs.[8] Molecular dynamics simulations by Savin and Kivshar have demonstrated that graphene nanoribbons can support vibrational localized states in the form of surface solitons and breathers.[9] The void ordering, observed in a number of metals and alloys under neutron and heavy-ion irradiations, was shown to be possible through the excitation of DBs.[17] DBs can assist structural transformations in stretched carbon nanotubes[18] and cause anomalies in charge diffusion.[24]

In the latest numerical studies, realistic interatomic potentials are used instead of considering the simplest types of anharmonicities and nearest-neighbor interactions. Diatomic crystals with realistic long-range interactions typically demonstrate a soft type of anharmonicity,[7,10–12,25–28] when the frequency of the DB decreases with the increase in its amplitude. In such crystals DBs can exist only in the presence of a forbidden band in the phonon spectrum, and they are called gap DBs.[29–33] Recently, a DB with frequency above the phonon band has been found numerically in graphene.[20]

In this paper we continue our studies of gap DBs in a two-dimensional crystal of A_3B composition with long-range Morse interactions.[10,25,26] For various temperatures, with the use of molecular dynamics, we measure the lifetime of high-energy atoms. Two atomic weight ratios, M_B/M_A, are considered. In one case the crystal supports gap DBs, and in the other case there are no DBs in the crystal due to the absence of the gap in the phonon spectrum. We also analyze the mechanisms of thermally activated formation of vacancy and interstitial atom pairs (Frenkel pairs) to understand the possible role of gap DBs in this process.

The paper is organized as follows. In Sec. II we briefly describe the simulation details. Sec. III A contains the description of how the atomic weight ratio affects the phonon density of states of the diatomic crystal and the existence of gap DBs. Section III B discusses the power spectra and the statistics of high-energy heavy and light atoms in the crystal at thermal equilibrium. In the Appendix, the mechanisms of Frenkel pair formation and the possible role of DBs in this process are investigated. Section IV concludes the paper.

II. SIMULATION DETAILS

We consider a two-dimensional crystal having A_3B stoichiometry, which is based on a hexagonal lattice and represents

the (111) plane of a three-dimensional crystal with $L1_2$ superstructure based on the face-centered-cubic lattice. A two-component crystal was chosen because it allows the possibility to change the width of the phonon gap simply by changing atomic weights of the components. Parameters of the Morse interatomic potentials used in our simulations can be found in the literature.[10,25,34] For the cutoff radius of the potential of 16 Å, the equilibrium lattice parameter was found to be $a = 2.60$ Å. For the atomic weight of atoms of type A we used $M_A = 9.75 \times 10^{-26}$ kg and for the atomic weight of atoms of type B we took two values corresponding to the atomic weight ratios $M_B/M_A = 0.46$ and $M_B/M_A = 0.10$. Thus, atoms A (B) are the heavy (light) atoms.

The computational cell used in our simulations included 32×32 primitive cells, and it was subjected to periodic boundary conditions. According to the considered stoichiometry, each primitive cell includes three atoms of type A and one atom of type B. Equations of motion for the atoms were integrated numerically using the sixth-order Störmer method with a time step of 0.1 fs.

In setting the initial conditions, we aimed to obtain a crystal at thermal equilibrium. For the computational cell with N degrees of freedom we summed all N linear phonon modes, choosing their amplitudes to share the total energy of the crystal equally between all the modes. This method of setting initial conditions does not take into account the interaction between phonon modes induced by the nonlinearity of the considered system. That is why this procedure was followed by thermalization during 100 ps. After that the analysis of thermal fluctuations in the crystal was carried out within 200 ps. Thermal expansion of the crystal was taken into account and all simulations were conducted at zero pressure.

In what follows, the temperature of the crystal is characterized by spatially (over ensemble) and temporally (over 0.18 ps $\approx 3\Theta$, where Θ is the DB's period) averaged kinetic energy per atom, $\overline{K}$. The temperature in a d-dimensional crystal (in our case $d = 2$) is related to $\overline{K}$ as

$$T = \frac{2}{d}\frac{\overline{K}}{k_B}, \tag{1}$$

where $k_B = 8.617 \times 10^{-5}$ eV K^{-1} is the Boltzmann constant.

Properties of gap DBs in thermal equilibrium were studied for the set of energies $\overline{K} = \{0.025, 0.05, 0.075, 0.1, 0.125\}$ eV. Corresponding temperatures are $T = \{290, 580, 870, 1160, 1450\}$ K. Higher energies were not considered because the waiting time of Frenkel pair formation becomes comparable to the duration of the numerical run (200 ps), but here we were interested in the statistics of high-energy atoms in a perfect crystal. Smaller energies were not considered because in this case it is problematic to reach thermal equilibrium within a reasonable simulation time.

The formation of Frenkel pairs (vacancy and interstitial atom pairs) was investigated for higher energies, $0.145 \leqslant \overline{K} \leqslant 0.167$ eV (temperatures $1683 \leqslant T \leqslant 1938$ K), after instantaneous heating from $\overline{K} = 0.13$ eV by rescaling the velocities of all atoms. After such heating, a certain time is needed for the system to reach thermal equilibrium. That is why we did not take energies higher than $\overline{K} = 0.167$ eV; otherwise, the Frenkel pairs appear in the system very quickly, before the thermal equilibrium is reached. For the highest temperature used in our study, i.e., for $\overline{K} = 0.167$ eV, the averaged waiting time of Frenkel pair formation was a few hundreds of DB periods and this was assumed to be sufficient for the system to reach thermal equilibrium. We assume that a Frenkel pair is formed if a pair of neighboring atoms move apart by more than 4.2 Å, which should be compared to the lattice parameter, $a = 2.6$ Å.

Phonon densities of states (DOS) were calculated at 0 K as described in our recent work.[10] Power spectra at finite temperatures were calculated from the Fourier transform of the autocorrelation function of atomic displacements, as described in detail in Ref. 23.

III. NUMERICAL RESULTS

A. Phonon spectra and DBs at zero temperature

According to our earlier studies,[10,25] for the atomic weight ratio $M_B/M_A = 0.10$, the considered crystal supports DBs and one example of DB at 0 K is given in Fig. 1. In Fig. 1(a), the stroboscopic picture presents the dynamics of atoms in the vicinity of a DB. Open (solid) circles correspond to heavy (light) atoms. Displacements of the atoms from lattice positions are multiplied by a factor of 4.

Phonon DOS calculated at 0 K are presented in Fig. 2(a) for $M_B/M_A = 0.10$ and in Fig. 3(a) for $M_B/M_A = 0.46$. In the former case the forbidden band in the phonon spectrum is $8.3 < \omega < 17.0$ THz, while for $M_B/M_A = 0.46$ there is no gap in the phonon spectrum and, consequently, the gap DBs do not exist.

The DB's frequency as a function of its amplitude, A, is shown in Fig. 1(b). The horizontal line indicates the upper edge of the phonon gap [cf. Fig. 2(a)]. It can be seen that the DB's frequency lies in the forbidden band of the phonon spectrum, closer to its upper edge, and it decreases with the increase in the

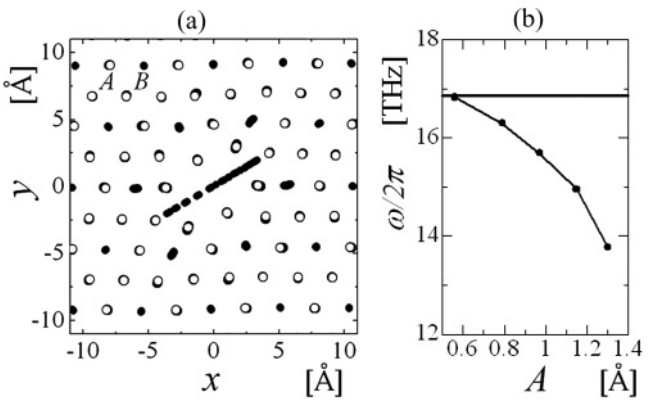

FIG. 1. (a) Stroboscopic picture of atomic displacements in the vicinity of gap DB in the crystal with atomic weight ratio $M_B/M_A = 0.10$. Open (solid) circles correspond to heavy (light) atoms. Displacements of atoms are multiplied by a factor of 4. (b) DB frequency as the function of its amplitude for $M_B/M_A = 0.10$ at zero temperature. The horizontal line indicates the upper edge of the phonon gap [cf. Fig. 2(a)].

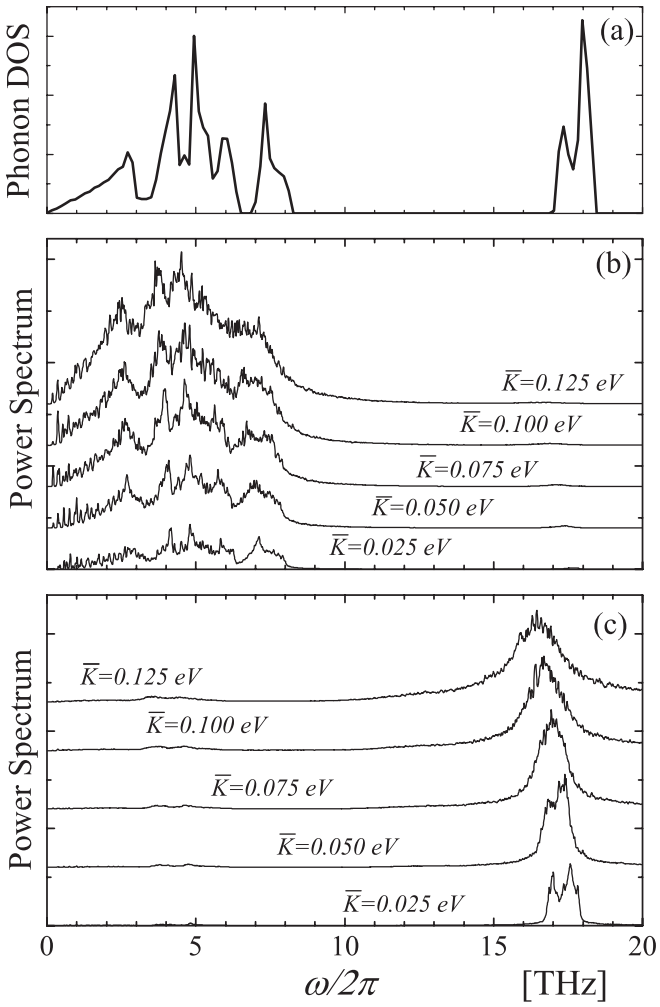

FIG. 2. (a) Phonon DOS calculated at 0 K. Power spectra for (b) heavy and (c) light atoms for different levels of kinetic energy, $\overline{K}$. Results for the atomic weight ratio $M_B/M_A = 0.10$.

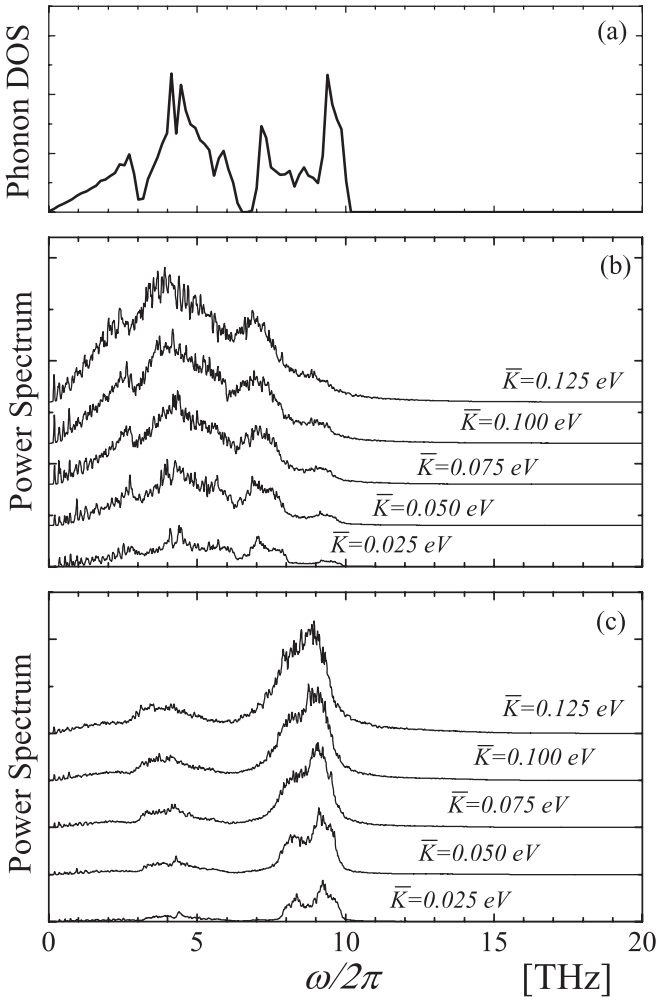

FIG. 3. Same as in Fig. 2, but for the atomic weight ratio $M_B/M_A = 0.46$.

DB's amplitude, varying in the range $13.7 < \omega_{\mathrm{DB}} < 16.8$ THz. Thus, the DB's period is about $\Theta = 0.06$ ps. In our study devoted to DB it is natural to measure time in DB periods, Θ.

B. Discrete breathers at thermal equilibrium

For a crystal at a given energy (temperature), we calculate power spectra and present the results in Figs. 2(b) and 2(c) for the atomic weight ratio $M_B/M_A = 0.10$, and in Figs. 3(b) and 3(c) for $M_B/M_A = 0.46$. In Figs. 2(b) and 3(b), the power spectra are shown for heavy atoms, and in Figs. 2(c) and 3(c), they are shown for light atoms. Naturally, the light atoms vibrate at higher frequencies than the heavy ones. Power spectra at the lowest studied energy, $\overline{K} = 0.025$ eV, are very close to the DOS calculated at 0 K and presented in Figs. 2(a) and 3(a). With increase in temperature, the most prominent change of the power spectra takes place for the high-frequency modes exhibited by the light atoms in Fig. 2(c), where considerable shift to the lower-frequency range can be easily seen. This shift can be explained by the excitation of DBs, nonlinear vibrational modes with the amplitude-dependent frequency [see Fig. 1(b)]. At higher temperatures DBs with higher amplitudes and hence with lower frequencies are excited. In Fig. 3(c) the redshift of the high-frequency vibrations at higher temperatures is practically absent because gap DBs cannot exist in this case.

We then analyze kinetic energies of heavy and light atoms, $K_{A,n}$ and $K_{B,n}$, averaged over 0.18 ps $\approx 3\Theta$. Atoms with $K_{A,n}, K_{B,n} > e\overline{K}$ are considered high-energy atoms, where $\overline{K}$ is the average over time and ensemble kinetic energy per atom and $e \approx 2.72$ is the base of the natural logarithm.

We are interested in the lifetime of high-energy atoms and their energies averaged over the lifetime, and we calculate these quantities separately for heavy and light atoms. An example of the time evolution of the relative kinetic energy of a particular light atom, $K_{B,n}/\overline{K}$, is presented in Fig. 4, where time is measured in the units of the DB's oscillation period, Θ. The horizontal dashed line indicates the level of kinetic energy equal to $K_{B,n}/\overline{K} = e$. In the present case $M_B/M_A = 0.10$ and $\overline{K} = 0.1$ eV. Referring to Fig. 4, we denote the lifetime of the high-energy state of the atom as t^*/Θ and the relative kinetic energy of this light atom averaged over time t^*/Θ as $K^*_{B,n}/\overline{K}$. In this example the lifetime of the atom in a high-energy state is $t^*/\Theta \approx 70$ and the average over the lifetime energy is $K^*_{B,n}/\overline{K} \approx 5.1$. Analogously we analyze high-energy heavy atoms.

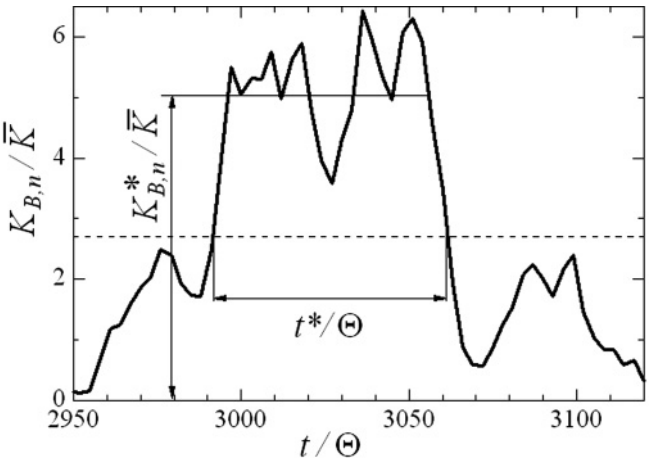

FIG. 4. Relative kinetic energy of particular light atom, $K_{B,n}/\overline{K}$, as a function of dimensionless time, t/Θ, where $\Theta = 0.06$ ps is the DB's period. The kinetic energy of the light atom, $K_{B,n}$, was averaged over time 0.18 ps $\approx 3\Theta$. The horizontal dashed line indicates the level of kinetic energy equal to $e\overline{K}$, where $e \approx 2.7$ is the base of the natural logarithm. The lifetime of the high-energy state of the atom is t^*/Θ, and its kinetic energy averaged over the lifetime is $K^*_{B,n}/\overline{K}$. Here the lifetime of the high-energy state is $t^*/\Theta \approx 70$ and its averaged energy is $K^*_{B,n}/\overline{K} \approx 5.1$. Results are for $M_B/M_A = 0.10$ and $\overline{K} = 0.1$ eV.

Concentrations of heavy and light high-energy atoms were defined as

$$C^*_A = \frac{n_A}{N_A N_{\rm obs}}, \quad C^*_B = \frac{n_B}{N_B N_{\rm obs}}, \tag{2}$$

where n_A (n_B) is the number of appearances of high-energy heavy (light) atoms in the computational cell during a numerical run of 200 ps, $N_A = 32 \times 32 \times 3 = 3072$ ($N_B = 32 \times 32 \times 1 = 1024$) is the number of heavy (light) atoms, and $N_{\rm obs} = 1111$ is the number of observations of the system during the numerical run.

In Fig. 5 we present numerical results for high-energy states of light and heavy atoms at thermal equilibrium for the atomic weight ratio $M_B/M_A = 0.10$. Figures 5(a)–5(e) correspond to the energies $\overline{K} = \{0.025,\ 0.05,\ 0.075,\ 0.1,\ 0.125\}$ eV, respectively. In Figs. 5(a)–5(e), for all high-energy heavy atoms observed during the numerical run, we show how the relative energy of the atoms in a high-energy state, $K^*_A/\overline{K}$, is related to the lifetime of this state, t^*/Θ. In Figs. 5(a′)–5(e′), the same is given for light atoms. In Figs. 5(a″)–5(e″), we present the concentrations of high-energy heavy atoms, C^*_A (thick line), and of high-energy light atoms, C^*_B (thin line), as the functions of their lifetime, t^*/Θ. Note that the ordinate is given in logarithmic scale.

In Fig. 6, we give the same as in Fig. 5 but for the atomic weight ratio $M_B/M_A = 0.46$. A remarkable difference in the results presented in Figs. 5 and 6 is that in the latter case they do not depend on temperature, whereas in the former one the results for the light high-energy atoms are temperature dependent, though for the heavy atoms the result is practically unchanged.

The qualitative difference in the results presented for the crystals with the atomic weight ratios $M_B/M_A = 0.10$ and $M_B/M_A = 0.46$ can only be explained through excitation of gap DBs at thermal equilibrium in the former case and their absence in the latter case. The following facts are in favor of this conclusion:

(1) Calculation of the power spectrum at thermal equilibrium has demonstrated that the main oscillation frequency of light atoms in the crystal with $M_B/M_A = 0.10$ at elevated temperatures lies in the gap of the phonon DOS, close to its upper edge [see Figs. 2(a) and 2(c)]. This is the feature of a

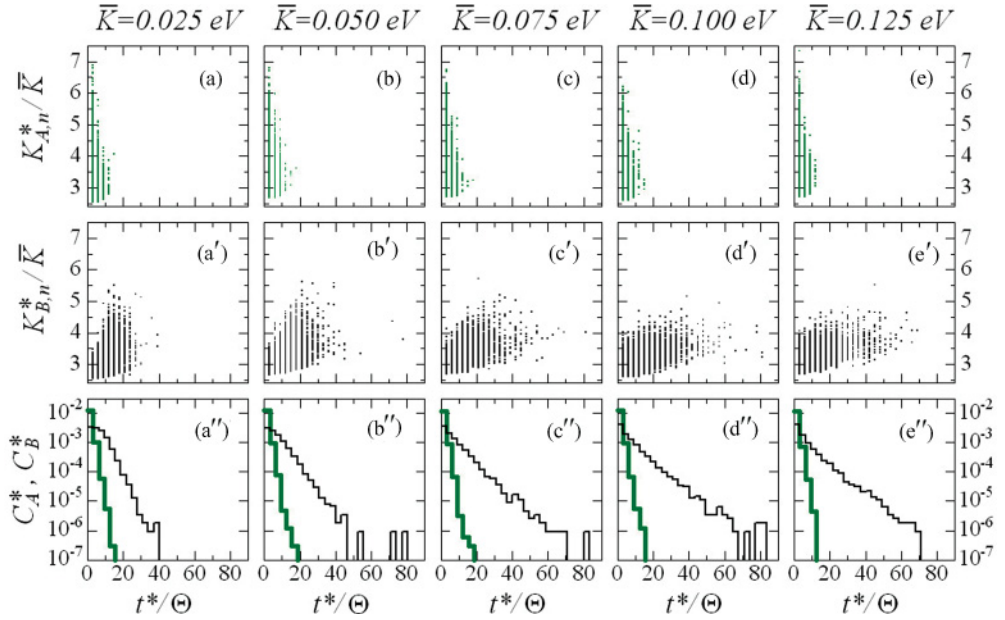

FIG. 5. (Color online) Characteristics of high-energy atoms in the crystal with atomic weight ratio $M_B/M_A = 0.10$. Rows correspond to five energies, $\overline{K} = \{0.025, 0.05, 0.075, 0.1, 0.125\}$ eV. (a)–(e) Relative energy of heavy atoms in high-energy state, $K^*_{A,n}/\overline{K}$, as a function of lifetime of this state, t^*/Θ; (a′)–(e′) same as in (a)–(e), but for light atoms; (a″)–(e″) concentrations of high-energy heavy atoms, C^*_A (thick line), and high-energy light atoms, C^*_B (thin line), as functions of their lifetime, t^*/Θ. The ordinate is given in logarithmic scale.

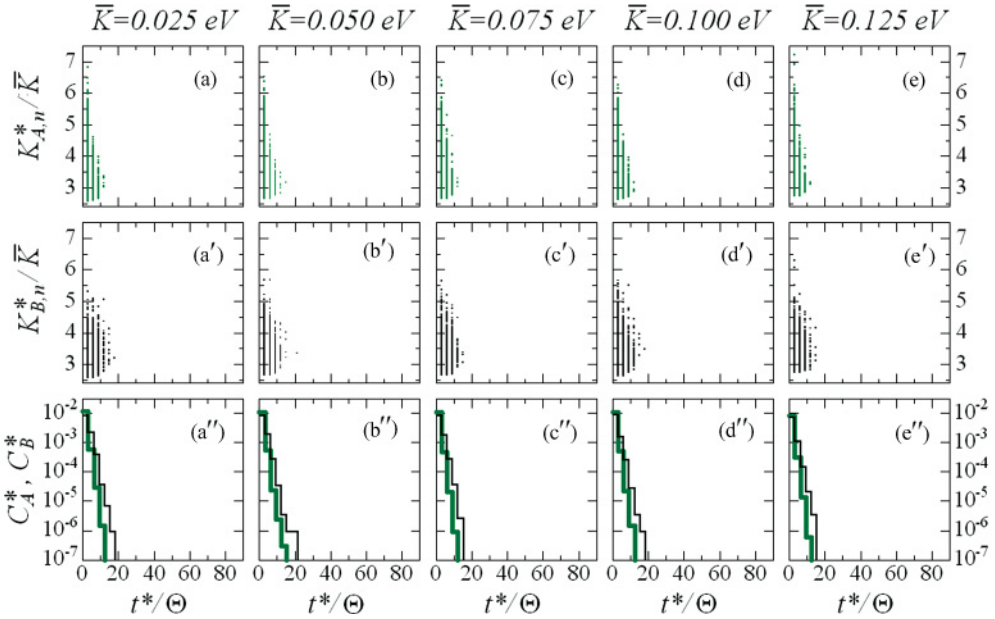

FIG. 6. (Color online) Same as in Fig. 5 but for the atomic weight ratio $M_B/M_A = 0.46$.

gap DB, whose frequency lies in the phonon gap and decreases with the increase in its amplitude [see Fig. 1(b)].

(2) The lifetime of high-energy light atoms increases with the increase in averaged energy, $\overline{K}$, in the crystal with $M_B/M_A = 0.10$, as one can see from Figs. 5(a″)–5(e″). This is in agreement with the fact that the contribution of DBs to the vibrational spectrum of the crystal increases with temperature, as DBs are essentially nonlinear vibrational modes.

(3) The increase in the lifetime of high-energy atoms with energy is observed in the crystal with $M_B/M_A = 0.10$ only for light but not for heavy atoms; cf. Figs. 5(a)–5(e) and 5(a′)–5(e′). This is consistent with the fact that only light atoms have large vibrational amplitudes in DBs, which is clearly seen from Fig. 1(a).

We thus conclude that the high-energy light atoms with large lifetime in the crystal with $M_B/M_A = 0.10$ can be identified as gap DBs.

From Figs. 5(a″)–5(e″) and 6(a″)–6(e″) one can see that in the semilogarithmic coordinates the concentration of high-energy atoms, C^*, at given energy, $\overline{K}$, is a linear function of their dimensionless lifetime, t^*/Θ. Then the following fitting dependence can be offered:

$$C^*_S = D \exp\left[-\alpha_S(\overline{K})\frac{t^*}{\Theta}\right], \quad S = \{A, B\}, \tag{3}$$

with a parameter $D > 0$ and energy-dependent coefficient α.

In Fig. 7 we present the dependence of coefficient α on energy $\overline{K}$ in the double logarithmic scale for $M_B/M_A = 0.46$ [Fig. 7(a)] and $M_B/M_A = 0.10$ [Fig. 7(b)]. Open (solid) circles present the results for heavy (light) components of the crystal. These results were obtained by least-squares fit of the curves in Figs. 5(a″)–5(e″) and 6(a″)–6(e″). Parameter α depends on temperature $\overline{K}$ only for the light atoms in the crystal with $M_B/M_A = 0.10$. The slope of the solid line in Fig. 7(b) is equal to $-1/2$ and it well approximates the numerical results for this case.

We conclude that, in the crystal with $M_B/M_A = 0.46$, not supporting gap DBs, the coefficient α in Eq. (3) does not depend on $\overline{K}$ for both heavy and light atoms:

$$\alpha_A(\overline{K}) = \text{const}, \quad \alpha_B(\overline{K}) = \text{const}. \tag{4}$$

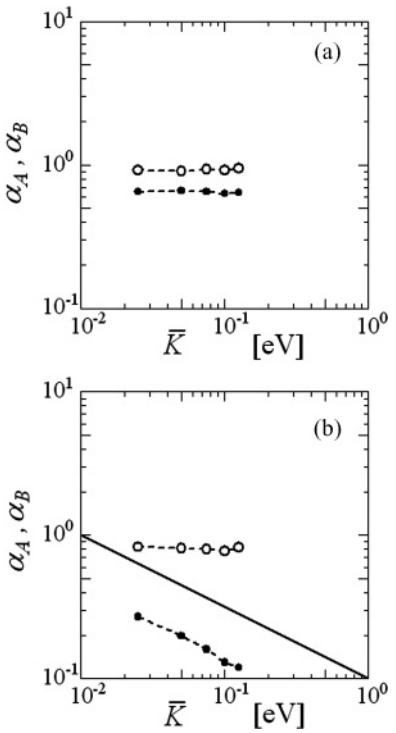

FIG. 7. Coefficient α of Eq. (3) as the function of energy, $\overline{K}$, in the double logarithmic scale for (a) $M_B/M_A = 0.46$ and (b) $M_B/M_A = 0.10$. Open (solid) circles show the results for heavy (light) atoms. Slope of the solid line in (b) is equal to $-1/2$ and it well approximates the numerical results for the light atoms.

On the other hand, in the crystal with $M_B/M_A = 0.1$, supporting gap DBs,

$$\alpha_A(\overline{K}) = \text{const}, \quad \alpha_B(\overline{K}) \sim \overline{K}^{-1/2}. \tag{5}$$

Equation (3), taken together with the second expression in Eq. (5), means that, in the crystal supporting DBs, the concentration of light high-energy atoms with a certain lifetime increases with energy (temperature).

IV. CONCLUSIONS

Molecular dynamics study of a two-dimensional diatomic crystal having stoichiometry A_3B was carried out at *thermal equilibrium* for two values of the atomic weight ratios, $M_B/M_A = 0.10$ and $M_B/M_A = 0.46$. In our previous study[10] it was demonstrated that at *zero temperature* the crystal with $M_B/M_A = 0.10$ supports gap DBs, in contrast to the crystal with $M_B/M_A = 0.46$. Two major issues were addressed in the present study: (i) the lifetime and energy of the high-energy atoms in the two crystals at different energies (temperatures) and (ii) the possible role of gap DBs in thermally activated formation of Frenkel pairs, i.e., vacancy and interstitial atom pairs (see Appendix).

The results can be summarized as follows.

(1) In the crystal not supporting DBs (atomic weight ratio $M_B/M_A = 0.46$), the concentrations of high-energy heavy atoms, C_A^*, and light atoms, C_B^*, do not depend on temperature. For the case of $M_B/M_A = 0.10$, when the crystal supports gap DBs, the situation for heavy atoms is the same, but the concentration of the high-energy light atoms, C_B^*, increases with temperature as described by Eqs. (3) and (5). The increase of concentration of the high-energy light atoms with temperature is attributed to excitation of DBs, essentially nonlinear localized vibrational modes. In our simulations, DBs with a lifetime of the order of 100Θ, where Θ is the DB's oscillation period, were observed at temperatures when Frenkel pairs start to form in the computational cell within the numerical run of 200 ps. In the crystal not supporting DBs, as well as in the sublattice of heavy atoms in the crystal supporting DBs, the lifetime of high-energy atoms is one order of magnitude smaller and it does not depend on temperature.

(2) The waiting time for point defect nucleation decreases exponentially with increase in temperature in both crystals, supporting and not supporting gap DBs. No contribution of gap DBs to the formation of Frenkel pairs was found; i.e., the waiting time for defect nucleation, within the simulation accuracy, was the same in the crystals with $M_B/M_A = 0.10$ and $M_B/M_A = 0.46$. Our results are in favor of cooperative motion of atoms as the major mechanism of thermally activated Frenkel pair formation.

In a forthcoming publication we address the issue of the temperature effect on structural instability of an elastically strained crystal supporting DBs.[35] We believe that DBs can trigger structural instabilities in strained crystals.

ACKNOWLEDGMENTS

The authors gratefully acknowledge the financial support provided by the Russian Foundation for Basic Research, Grant No. 11-08-97057-r_povolzhie_a.

APPENDIX: THERMALLY ACTIVATED FORMATION OF FRENKEL PAIRS

In Sec. III B the existence (absence) of DBs in thermal equilibrium was confirmed for a crystal with $M_B/M_A = 0.10$ ($M_B/M_A = 0.46$). In the crystal supporting DBs, the lifetime of light atoms in a high-energy state increases with energy $\overline{K}$. It is interesting to check if DBs can influence the frequency of Frenkel pair formation.

In this simulation we take an ideal crystal thermalized at $\overline{K} = 0.13$ eV and then instantly increase temperature up to a value from the range $0.145 \leqslant \overline{K} \leqslant 0.167$ eV by rescaling velocities of all atoms.

In Fig. 8 we show the relation between the dimensionless waiting time of Frenkel pair formation, t_w/Θ, where Θ is the period of the DB, and energy $\overline{K}$. The ordinate is presented in logarithmic scale. Results for the crystal with $M_B/M_A = 0.10$ are shown by open squares, and results for the crystal with $M_B/M_A = 0.46$ by solid diamonds. Each point is a result of averaging over 10 numerical runs. The results of least-squares fit of the numerical data are shown by solid (dashed) lines for the crystals with large (small) atomic weight ratio.

It is well seen from Fig. 8 that the difference in the slopes of fitting lines lies within the accuracy of the calculations. Thus, we conclude that in both cases the waiting time of Frenkel pair formation, t_w, decreases exponentially with increase in energy and that the existence of DBs in the system does not affect the waiting time of Frenkel pair formation.

Visual analysis of the atomic displacements at the moment of Frenkel pair formation has revealed that the major role in this process is played by the collective modes of atomic displacements.[36] The cooperation of the atomic motion

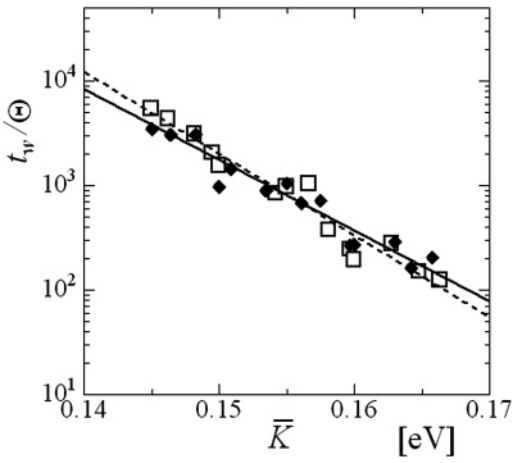

FIG. 8. Waiting time of Frenkel pair nucleation vs energy. Open squares correspond to the crystal with $M_B/M_A = 0.10$ and solid diamonds to the crystal with $M_B/M_A = 0.46$. Each point is a result of averaging over 10 numerical runs. Fitting lines are shown by solid (dashed) lines for crystals with large (small) atomic weight ratios.

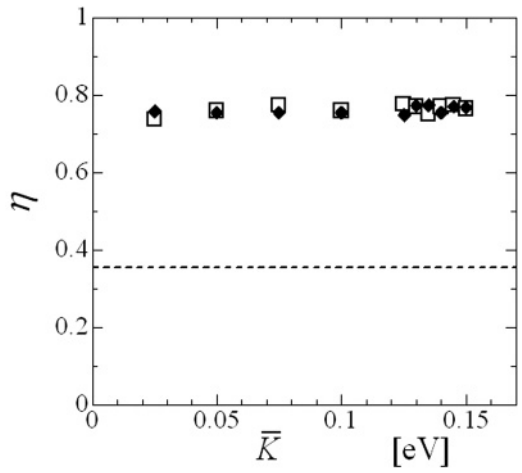

FIG. 9. Cooperative factor, η, as a function of energy, $\overline{K}$. The results of the crystal with $M_B/M_A = 0.10$ are shown by open squares, and solid diamonds correspond to the crystal with $M_B/M_A = 0.46$. The horizontal dashed line shows the level of $\eta = 0.356$, corresponding to random atomic displacements.

can be quantified by the following cooperative factor of atomic displacements,[36]

$$\eta = \frac{1}{N}\sum_{i=1}^{N} \frac{\sqrt{\left(\sum_{j=1}^{n_i} \Delta x_j\right)^2 + \left(\sum_{j=1}^{n_i} \Delta y_j\right)^2}}{\sum_{j=1}^{n_i} \sqrt{\Delta x_j^2 + \Delta y_j^2}}, \qquad \text{(A1)}$$

where N is the number of atoms in the computational cell, n_i is the number of atoms in a microscopic atomic cluster around the ith atom (in our simulations, the cluster included the ith atom itself and its six nearest neighbors, i.e., we had $n_i = 7$), and Δx_j, Δy_j are components of displacement of the jth atom from its equilibrium position. One can see that $\eta = 1$ if all atoms have the same displacement vector. If Δx_j and Δy_j are random numbers homogeneously distributed in the range $[-1,1]$, then, for a two-dimensional (2D) crystal and for $n_i = 7$, the cooperative factor is $\eta = 0.356$.

In Fig. 9 we give the cooperative factor, η, as a function of energy, $\overline{K}$. The results for the crystal with $M_B/M_A = 0.10$ are shown by open squares, and solid diamonds correspond to the crystal with $M_B/M_A = 0.46$. The horizontal dashed line shows the level of $\eta = 0.356$, corresponding to random atomic displacements. As one can see, in both crystals, values of η lie substantially above the dashed line, indicating the cooperative character of atomic displacements. Remarkably, the cooperative factor η does not depend on temperature and it is not affected by the presence of DBs in the crystal with $M_B/M_A = 0.10$. We note that the value $\eta = 0.76$ reported by the authors of Ref. 36 for 2D crystals of pure copper, aluminum, and nickel is in excellent agreement with the result presented in Fig. 9. Thus, parameter η appears to be a conserved quantity that, for a given lattice, depends neither on temperature nor on the crystal composition. We conclude that cooperative motion of atoms in thermal equilibrium is more important for thermally activated formation of Frenkel pairs than the presence or absence of DBs.

[1] S. Flach and A. V. Gorbach, Phys. Rep. **467**, 1 (2008).
[2] M. E. Manley, Acta Mater. **58**, 2926 (2010).
[3] S. Flach and C. R. Willis, Phys. Rep. **295**, 181 (1998).
[4] D. K. Campbell, S. Flach, and Yu. S. Kivshar, Phys. Today **57**, 43 (2004).
[5] M. E. Manley, A. J. Sievers, J. W. Lynn, S. A. Kiselev, N. I. Agladze, Y. Chen, A. Llobet, and A. Alatas, Phys. Rev. B **79**, 134304 (2009).
[6] M. E. Manley, D. L. Abernathy, N. I. Agladze, and A. J. Sievers, Sci. Rep. **1**, 4 (2011).
[7] S. A. Kiselev and A. J. Sievers, Phys. Rev. B **55**, 5755 (1997).
[8] A. R. Bishop, A. Bussmann-Holder, S. Kamba, and M. Maglione, Phys. Rev. B **81**, 064106 (2010).
[9] A. V. Savin and Yu. S. Kivshar, Europhys. Lett. **89**, 46001 (2010).
[10] S. V. Dmitriev, A. A. Sukhorukov, A. I. Pshenichnyuk, L. Z. Khadeeva, A. M. Iskandarov, and Yu. S. Kivshar, Phys. Rev. B **80**, 094302 (2009).
[11] L. Z. Khadeeva and S. V. Dmitriev, Phys. Rev. B **81**, 214306 (2010).
[12] S. V. Dmitriev, N. N. Medvedev, R. R. Mulyukov, O. V. Pozhidaeva, A. I. Potekaev, and M. D. Starostenkov, Russ. Phys. J. **51**, 858 (2008).
[13] Yu. S. Kivshar and G. P. Agrawal, *Optical Solitons: From Fibers to Photonic Crystals* (Academic, New York, 2003).
[14] A. E. Miroshnichenko, S. Flach, M. V. Fistul, Y. Zolotaryuk, and J. B. Page, Phys. Rev. E **64**, 066601 (2001).
[15] T. Dauxois, M. Peyrard, and A. R. Bishop, Phys. Rev. E **47**, 684 (1993).
[16] F. Kh. Abdullaev, B. B. Baizakov, S. A. Darmanyan, V. V. Konotop, and M. Salerno, Phys. Rev. A **64**, 043606 (2001).
[17] V. Dubinko, Nucl. Instrum. Methods Phys. Res., Sect. B **267**, 2976 (2009).
[18] T. Shimada, D. Shirasaki, and T. Kitamura, Phys. Rev. B **81**, 035401 (2010).
[19] Y. Kinoshita, Y. Yamayose, Y. Doi, A. Nakatani, and T. Kitamura, Phys. Rev. B **77**, 024307 (2008).
[20] Y. Yamayose, Y. Kinoshita, Y. Doi, A. Nakatani, and T. Kitamura, Europhys. Lett. **80**, 40008 (2007).
[21] A. J. Sievers and S. Takeno, Phys. Rev. Lett. **61**, 970 (1988).
[22] M. V. Ivanchenko, O. I. Kanakov, V. D. Shalfeev, and S. Flach, Physica D **198**, 120 (2004).
[23] M. Eleftheriou and S. Flach, Physica D **202**, 142 (2005).
[24] G. Kalosakas, K. L. Ngai, and S. Flach, Phys. Rev. E **71**, 061901 (2005).
[25] S. V. Dmitriev, L. Z. Khadeeva, A. I. Pshenichnyuk, and N. N. Medvedev, Phys. Solid State **52**, 1499 (2010).
[26] S. V. Dmitriev, A. A. Nazarov, A. I. Potekaev, A. I. Pshenichnyuk, and L. Z. Khadeeva, Russ. Phys. J. **52**, 132 (2009).
[27] N. N. Medvedev, M. D. Starostenkov, P. V. Zakharov, and O. V. Pozidaeva, Tech. Phys. Lett. **37**, 98 (2011).

[28] S. V. Dmitriev and L. Z. Khadeeva, Phys. Solid State **53**, 1425 (2011).
[29] A. V. Gorbach and M. Johansson, Phys. Rev. E **67**, 066608 (2003).
[30] G. James and M. Kastner, Nonlinearity **20**, 631 (2007).
[31] A. V. Gorbach, A. S. Kovalev, and O. V. Usatenko, Phys. Solid State **43**, 2171 (2001).
[32] I. A. Butt and J. A. D. Wattis, J. Phys. A: Math. Theor. **40**, 1239 (2007).
[33] Y. Doi, A. Nakatani, and K. Yoshimura, Phys. Rev. E **79**, 026603 (2009).
[34] A. I. Tsaregorodtsev, N. V. Horlov, B. F. Demianov, and M. D. Starostenkov, Phys. Met. Metallogr. **58**, 336 (1984).
[35] S. V. Dmitriev and J. A. Baimova, Tech. Phys. Lett. **37**, 451 (2011); Tech. Phys. **56**, 1612 (2011).
[36] G. M. Poletaev and M. D. Starostenkov, Phys. Solid State **51**, 727 (2009).